THE JOURNAL OF BIOLOGICAL CHEMISTRY VOL. 287, NO. 15, pp. 11665–11676, April 6, 2012

Microcin Amyloid Fibrils A Are Reservoir of Toxic Oligomeric Species[S]

Received for publication, July 13, 2011, and in revised form, February 13, 2012 Published, JBC Papers in Press, February 15, 2012, DOI 10.1074/jbc.M111.282533

Mohammad Shahnawaz and Claudio Soto[1]

From the Mitchell Center for Alzheimer's Disease and Related Brain Disorders, Department of Neurology, University of Texas Houston Medical School, Houston, Texas 77030

Microcin E492 (Mcc), a low molecular weight bacteriocin produced by *Klebsiella pneumoniae* RYC492, has been shown to exist in two forms: soluble forms that are believed to be toxic to the bacterial cell by forming pores and non-toxic fibrillar forms that share similar biochemical and biophysical properties with amyloids associated with several human diseases. Here we report that fibrils polymerized *in vitro* from soluble forms sequester toxic species that can be released upon changing environmental conditions such as pH, ionic strength, and upon dilution. Our results indicate that basic pH (≥8.5), low NaCl concentrations (≤50 mM), and dilution (>10-fold) destabilize Mcc fibrils into more soluble species that are found to be toxic to the target cells. Additionally, we also found a similar conversion of non-toxic fibrils into highly toxic oligomers using Mcc aggregates produced *in vivo*. Moreover, the soluble protein released from fibrils is able to rapidly polymerize into amyloid fibrils under fibril-forming conditions and to efficiently seed aggregation of monomeric Mcc. Our findings indicate that fibrillar forms of Mcc constitute a reservoir of toxic oligomeric species that is released into the medium upon changing the environmental conditions. These findings may have substantial implications to understand the dynamic process of interconversion between toxic and non-toxic aggregated species implicated in protein misfolding diseases.

Bacteriocins are a group of polypeptide antibiotics excreted by different bacterial genera including Gram-negative and Gram-positive species (1–3). Once released, they restrain the growth of competing bacterial strains in a receptor-mediated manner employing several mechanisms. Mcc[2] is a low molecular weight (~7.8 kDa) bacteriocin produced by *Klebsiella pneumoniae* RYC492 (4–6). Antibacterial activity of Mcc appeared to be restricted to the *Enterobacteriaceae* species, closely related to the producer strain that directly competes with *Klebsiella* to occupy a spatial niche in the ecosystem (5, 7). Mcc has been shown to exert its toxic effect by forming ion channels on the cell membrane of target cells in a receptor-mediated fashion, which leads to a rapid depolarization and thus permeabilization of the cell membrane (6, 8, 9). Unlike other bacteriocins, toxic forms of Mcc are produced mainly in the exponential phase and comparatively less toxic in the stationary phase (5, 10). Surprisingly, neither apparent differences in the amounts of Mcc nor degradation or post-translational modifications have been shown to be responsible for the loss of activity (11). Some reports have described that these changes in Mcc toxicity may be due to the production of a microcin antagonist known as enterochelin in the stationary phase (12). More recently, the loss of Mcc toxicity in the stationary phase has been attributed to changes in the folding and polymerization of Mcc into aggregated structures similar to amyloid fibrils (13). Compelling *in vitro* and *in vivo* studies have shown that the changes on the Mcc activity during the bacterial life cycle is due to the conversion of toxic soluble Mcc (produced in the exponential phase) into non-toxic amyloid-like fibrils (produced in stationary phase) (13). These results are intriguing as they suggest that amyloid formation once thought to be exclusively associated with human diseases (such as Alzheimer, Parkinson, diabetes type II, and prion diseases) also plays a role on modulating the biological activity of proteins in such distant organisms as bacteria. There are many similarities between Mcc amyloid fibrils and those formed by disease-associated proteins, namely β-sheet-rich secondary structure, morphology under electron microscopy, binding to amyloid specific dies, protease resistance, and a seeding nucleation mechanism of polymerization (13). Furthermore, Mcc aggregates are also toxic to eukaryotic cells (14), and interestingly, the degree of toxicity is dependent upon the size of polymers; oligomers are highly toxic for both bacteria and eukaryotic cells, and large fibrillar structures are little or non-toxic (13, 14). The latter is analogous to the widely accepted view in the field of protein misfolding disorders that soluble oligomers are the culprits of cell dysfunction, tissue damage, and disease, and the formation of large fibrils is likely a protective mechanism to encapsulate the toxic species (15).

Here we hypothesize that fibrils sequester toxic species of Mcc that could be released in the medium upon changing environmental conditions. To test this hypothesis, we investigated the stability of Mcc fibrils by changing three different conditions: pH, ionic strength, and dilution. The results indicate that *in vitro* or *in vivo* polymerized Mcc fibrils disaggregate into soluble species at basic pH (≥8.5), at low NaCl concentrations (≤50 mM), and upon dilution (10-fold). The released species were highly toxic to the bacterial cells. We also provide evidence that soluble proteins released from fibrils upon disaggregation are able to reassemble into mature fibrils, suggesting that the process of fibril formation and dissolution is highly dynamic and reversible. Our findings suggest that Mcc fibrils work as a

[S] This article contains supplemental Figs. S1 and S2.

[1] To whom correspondence should be addressed: University of Texas Houston Medical School, 6431, Fannin St., Houston, TX 77030. Tel.: 713-5007086; E-mail: Claudio.Soto@uth.tmc.edu.

[2] The abbreviations used are: Mcc, microcin E492; ThT, thioflavin T; SEC, size exclusion chromatography; Bis-Tris, 2-[bis(2-hydroxyethyl)amino]-2-(hydroxymethyl)propane-1,3-diol.

reservoir of releasable toxic species. These results may have important consequences to understand microbial homeostasis in the natural ecosystem and might be extrapolated to the behavior of disease associated amyloid aggregates.

EXPERIMENTAL PROCEDURES

Chemicals were obtained from Sigma unless otherwise stated.

Purification of Mcc—Mcc was purified from the culture supernatants as described earlier (13). In brief, *Escherichia coli* VCS257 cells harboring pJEM15 plasmid were grown in M9 minimal medium containing 0.2% glucose, 0.2% sodium citrate, 1 g/liter casamino acid, 1 mg/liter thiamine, and 100 mg/liter ampicillin to an absorbance of 1.2 at 600 nm at 37 °C with shaking. Bacterial cell debris was removed by centrifugation at 4000 rpm for 10 min. The resultant supernatant was passed through a Sep-Pak C18 cartridge (Waters). The cartridge was sequentially washed with 65% methanol and 25% acetonitrile. Finally, the bound Mcc was eluted with 50% acetonitrile and lyophilized. Lyophilized powder of Mcc was stored at −20 °C until used. Under these conditions, the preparation contains highly purified Mcc (>90%) as evaluated by silver-stained gels (16).

Mcc Aggregation and Fibril Disaggregation—To start Mcc aggregation, lyophilized Mcc powder was dissolved in sterile 10 mM NaOH solution and filtered through a 30-kDa cutoff filter to remove aggregates. The protein concentration in the filtrate (considered as monomers) was estimated by the BCA assay kit (Pierce) and used immediately or stored frozen at −80 °C. To prepare fibrils of Mcc, soluble protein was incubated at a concentration of 400 μg/ml in aggregation buffer (50 mM PIPES-NaOH, pH 6.5, 0.5 M NaCl) for 24 h at 37 °C with vigorous shaking. Fibril formation was characterized by thioflavin T (ThT) binding assay, turbidity, sedimentation assay, dot blots, size-exclusion chromatography, and electron microscopy.

For disaggregation of Mcc aggregates, fibrils formed after 24 h of incubation in aggregation buffer at 37 °C were centrifuged at 16,500 × *g* for 10 min. Then, preformed fibrils were treated for 2 h at 25 °C under three different conditions as follows: First, fibrils were incubated in buffers of different pH. Fibrils (400 μg/ml) were resuspended in the following buffers: 50 mM glycine, pH 2.5; 50 mM sodium acetate, pH 5.5; 50 mM PIPES, pH 6.5; 50 mM Tris, pH 7.5, 8.5, and 9.5; 50 mM sodium borate, pH 10.5 or 0.1% NH_4OH, pH 10.5 (in some cases where lyophilization was required). Each of these solutions contained 500 mM NaCl. Second, fibrils were incubated in buffers with different NaCl concentrations. Fibrils (400 μg/ml) were resuspended in 50 mM PIPES, pH 6.5, containing 0, 50, 150, 500, 750, and 1000 mM NaCl. 3). Third, the samples were submitted to different dilutions. Fibrils (400 μg/ml) were disaggregated upon dilutions (1-, 5,- and 10-fold) in 50 mM PIPES-NaOH, pH 6.5, containing 500 mM NaCl.

After 2 h of incubation with the new condition, samples were either used as such for turbidity assay, electron microscopy, and cytotoxicity studies, or samples were centrifuged at 16,500 × *g* for 10 min, and supernatants were used for dot blot analysis and protein estimation by a BCA protein assay kit. In all cases, untreated Mcc fibrils (control) were used in 50 mM PIPES, pH 6.5, containing 500 mM NaCl.

Reassembly of Released Mcc Oligomers and Seeding Aggregation of Fresh Soluble Mcc—Fibrils (400 μg/ml) were allowed to disaggregate by diluting 10-fold in 50 mM sodium borate, pH 10.5, 0 mM NaCl for 2 h at 25 °C. After incubation, sample was centrifuged at 16,500 × *g* for 10 min. The resultant soluble protein in supernatant was concentrated. For reassembly, concentrated protein was diluted in aggregation buffer to a final concentration of 400 μg/ml and incubated at 37 °C with vigorous shaking for 48 h. For seeding aggregation of fresh Mcc, fresh soluble Mcc (400 μg/ml) was incubated at 37 °C for 48 h either alone or with 20 or 40 μg/ml seed (released soluble protein from fibrils upon treatment at pH 10.5, 0 mM NaCl, and dilution 10-fold). Aliquots were removed at different time points, and ThT assay was carried out as described below.

Isolation of in Vivo Polymerized Mcc Fibrils from Bacterial Culture—VCS257 cells harboring pJEM15 were grown in M9 medium as described above at 37 °C for 48 h. Cells were removed by centrifugation at 4000 rpm for 10 min. Then, culture supernatants were centrifuged at 16,500 × *g* for 10 min. Pellet-containing Mcc fibrils were washed 2 times with aggregation buffer (50 mM PIPES, pH 6.5, containing 500 mM NaCl). The concentration of the fibrils was measured by the BCA assay kit. Disaggregation of *in vivo* polymerized Mcc fibrils was carried out in a similar manner as described for Mcc fibrils polymerized *in vitro* from purified soluble Mcc (see above).

Sedimentation Assay—Sedimentation was used to examine the extent of Mcc aggregation or Mcc fibrils disaggregation. After the aggregation or disaggregation experiments, samples were centrifuged at 16,500 × *g* for 10 min. Soluble proteins in the supernatant were collected in fresh tubes. The amount of Mcc in the supernatant was estimated by dot blot analysis, as described below. Total protein concentration in supernatants was estimated by the BCA assay kit.

Dot Blot Analysis—Five μl of each reaction was spotted onto nitrocellulose membranes (Amersham Biosciences) and air-dried for 30 min at room temperature. Membranes were blocked with 5% w/v nonfat dry milk in Tris-buffered saline-Tween 20 (TBS-T, 20 mM Tris, pH 7.2, 150 mM NaCl, and 0.05% (v/v) Tween 20) at room temperature for 2 h. After blocking, the membranes were probed with anti-Mcc antibody (1:3000) and the anti-rabbit horseradish peroxidase-conjugated secondary antibody (1:5000). The blots were visualized using enhanced chemiluminescence plus Western blotting detection kit (Amersham Biosciences).

Turbidity Assay—The amount of Mcc aggregates under various conditions was also assessed by turbidity assay. For that, the turbidity of each sample was monitored by measuring absorbance at 340 nm using UV-visible spectrometer (U-3900, HITACHI, Japan). In all cases, corresponding buffer solutions were used as blanks.

ThT Binding Assay—The kinetic of Mcc fibril formation was monitored by ThT binding assay as described (13). Mcc (400 μg/ml) was allowed to aggregate in 50 mM PIPES (pH 6.5) containing 500 mM NaCl at 37 °C with vigorous shaking for different times. At the end of the reaction, 20 μl of the reaction mixture was mixed with 80 μl of 6 μM ThT in 1× phosphate buffered saline solution, and fluorescence was measured immediately at excitation 435 nm and emission of 485 nm

using a microplate spectrofluoremeter Gemini-XS (Molecular Devices, Sunnyvale, CA).

Transmission Electron Microscopy—An aliquot of 10 μl of reaction sample was placed onto Formvar-coated 200-mesh copper grids for 5 min, washed at least 3 times with distilled water, and then negatively stained with 2% uranyl acetate for 1 min. Grids were examined by electron microscopy (H-7600, Hitachi, Japan) operated at an accelerating voltage of 80 kV.

Size Exclusion Chromatography (SEC)—The sizes of Mcc species formed during Mcc aggregation (400 μg/ml in 50 mM PIPES-NaOH, pH 6.5, 500 mM NaCl at 37 °C) and upon disaggregation of Mcc fibrils (400 μg/ml after diluting10-fold in 0.1% NH_4OH, pH 10.5, 0 mM NaCl at 25 °C) were analyzed by SEC. Aliquots were removed at various time points from Mcc aggregation reaction and from Mcc fibrils disaggregation reaction. All aliquots were centrifuged at 16,500 $\times$ *g* for 10 min to remove big aggregates, and soluble material in supernatants were subjected to SEC on a Superdex 200 10/300 GL (Amersham Biosciences) column using aggregation buffer (50 mM PIPES-NaOH, pH 6.5, 0.5 M NaCl) as the liquid phase at a flow rate of 0.25 ml/min at room temperature. The elution profiles were detected by absorbance at 280 nm. A molecular mass standard curve was constructed by measuring elution times of: thyroglobulin, 669 kDa; ferritin, 440 kDa; aldolase, 158 kDa; conalbumin, 75 kDa; ovalbumin, 44 kDa (all from Amersham Biosciences).

SDS-PAGE and Immunoblotting—Soluble Mcc species formed during Mcc aggregation and upon disaggregation of Mcc fibrils were analyzed by SDS-PAGE followed by immunoblotting. Samples were resolved by NuPAGE 4–12% Bis-Tris gels (Invitrogen). Proteins were electrophoretically transferred to nitrocellulose membranes (Amersham Biosciences). Membranes were blocked with 5% w/v nonfat dry milk in Tris-buffered saline, Tween 20 (TBS-T) at room temperature for 2 h. After blocking, the membranes were probed with anti-Mcc antibody (1:3000) and the anti-rabbit horseradish peroxidase-conjugated secondary antibody (1:5000). The blots were visualized using enhanced chemiluminescence plus Western blotting detection kit (Amersham Biosciences).

Antibacterial Activity—E. coli BL21(DE3)p11α2 cells were grown in Luria-Bertani (LB) medium at 37 °C to an absorbance (A_{600}) of 0.5–0.6. The cell suspension was diluted to an A_{600} of 0.001 ($\sim 5 \times 10^5$ colony-forming units/ml) in LB medium. Aliquots of 20 μl from untreated Mcc fibrils and Mcc fibrils treated at varying conditions as described above were withdrawn and mixed with 180 μl (from $\sim 5 \times 10^5$ colony-forming units /ml) of cell suspension. Tubes were incubated at 37 °C for 16 h without shaking. Cytotoxic effects of untreated and treated Mcc fibrils were evaluated by measuring bacterial growing through the absorbance at 600 nm using an Eppendorf Biophotometer.

RESULTS

Preparation and Characterization of Mcc Fibrils—Before starting disaggregation experiments it is important to have a well characterized preparation of Mcc amyloid fibrils. To obtain seed-free Mcc protein, lyophilized Mcc was resuspended in 10 mM NaOH and filtered through a 30-kDa cutoff. To prepare Mcc fibrils, soluble Mcc was incubated at 37 °C with shaking in 50 mM PIPES, pH 6.5, containing 500 mM NaCl. Aliquots were removed at different time points, and aggregation was determined by ThT binding assay (Fig. 1*A*), sedimentation assay followed by dot blotting (Fig. 1*B*), and electron microscopy (Fig. 1*C*). ThT binding assay showed a time-dependent increase in ThT fluorescence. Similarly a time-dependent decrease in the amount of soluble Mcc in the supernatant was observed by dot blot after sedimentation (Fig. 1*B*). Disappearance of soluble Mcc in the supernatant correlated with an increase in ThT fluorescence, suggesting the formation of β-sheet-rich aggregates able to bind to ThT. Electron microscopy of unaggregated sample (0 h) did not show any detectable structures. After 3 h of incubation, a scarce amount of small oligomers with diameters of ~2–30 nm could be observed (Fig. 1*C*). The quantity of these structures was higher after 6 h of incubation, in which some of the oligomers presented a larger size (~60 nm). Sample incubated for 9–12 h showed the predominant presence of ~100–300-nm long protofibrillar structures (Fig. 1*C*). Finally, after 24–48 h of incubation, samples were enriched in bundles of classical unbranched amyloid fibrils of variable length. In our previously published study we have shown that these structures are rich in β-sheet secondary structure and resistant to proteolytic degradation (13).

Disaggregation of Mcc Fibrils—A balance of electrostatic and hydrophobic interactions has been shown to be required for the formation and stability of amyloid fibrils (17, 18). To study the stability and reversibility of Mcc amyloid in the presence of environmental changes, preformed fibrils were incubated in buffers at different pH, ionic strengths (NaCl concentrations), or at distinct dilutions.

Effect of pH on Mcc Fibrils Disaggregation—To evaluate the effect of pH on Mcc fibrils stability, we treated preformed Mcc fibrils at varying pH (2.5, 5.5, 6.5, 7.5, 8.5, 9.5, and 10.5) for 2 h. The extent of disaggregation was assessed by sedimentation assay (Fig. 2, *A* and *B*), turbidity assay (Fig. 2*C*), and electron microscopy (Fig. 2*D*). The results from sedimentation assay (Fig. 2, *A* and *B*) show the amount of soluble protein in the supernatant increased proportionally when pH was increased from 8.5 to 10.5. Approximately 21% of the total protein was found in the soluble form when fibrils were treated at pH 10.5, whereas neither acidic pH (2.5–5.5) nor neutral pH (6.5–7.5) had any effect on fibril dissolution. Similarly, turbidity assay (Fig. 2*C*) revealed a significant decrease in turbidity of fibrils treated at pH 8.5 to 10.5, as compared with untreated Mcc fibrils (control) (Fig. 2*C*, *dashed line*). The increase of Mcc in the supernatant after centrifugation and the decrease in turbidity upon incubation at basic pH implies the conversion of large fibrillar structures into smaller species (oligomers and/or monomers). To determine the type of structures produced upon fibril dissolution at basic pH, we examined the samples under electron microscope after negative staining. No distinguishable changes were observed in fibrils at pH 2.5–7.5. However, a transition of mature fibrils into smaller structures was evident at pH 8.5, in which many shorter and thinner fibrils appeared (Fig. 2*D*). This trend was more pronounced at pH 9.5 and 10.5, resulting in the formation of heterogeneous species, with predominant formation of small globular oligomers similar to those described for disease-associated proteins (15, 19,

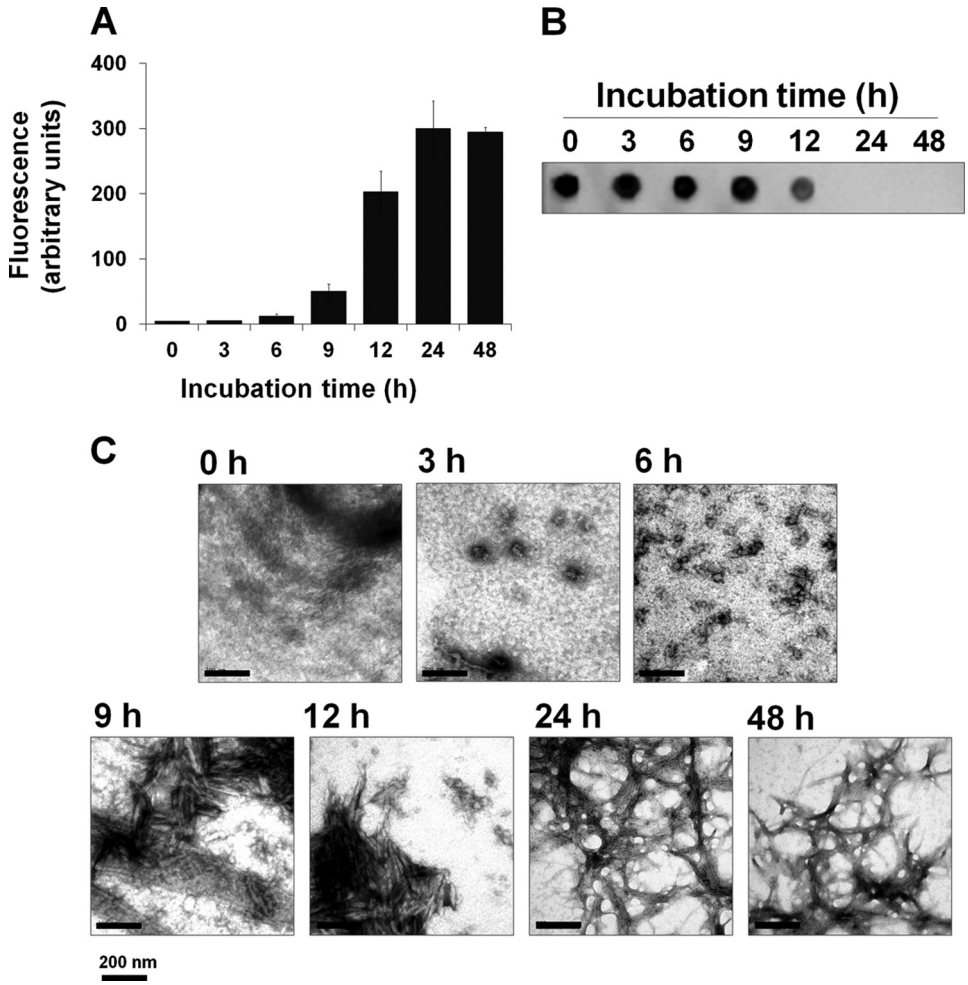

FIGURE 1. **Formation and characterization of Mcc fibrils *in vitro*.** Purified soluble Mcc at a concentration of 400 μg/ml was incubated in 50 mM PIPES-NaOH, pH 6.5, 500 mM NaCl at 37 °C with agitation for 0, 3, 6, 9, 12, and 24 h. Aliquots were removed at each time point, and samples were analyzed by ThT binding assay (*A*) to measure amyloid fibril formation and by quantitation by dot blot of Mcc remaining soluble after centrifugation at 16,500 × *g* for 10 min (*B*). *C*, electron microscopy images of negatively stained aliquots after each time point as indicated above were examined using a magnification of 150,000. *Bars* represent 200 nm. *Error bars* represent ± S.D. of triplicate samples.

20). These results indicate that basic pH (≥8.5) destabilize amyloid aggregates, promoting the conversion of large fibrils into smaller oligomeric species. SDS-PAGE of soluble Mcc at varying pH values showed the presence of large oligomers of molecular mass ~100 to >260 kDa and monomers through tetramers (<10 to ~30 kDa) (supplemental Fig. S1*A*). These species became more abundant as the pH increased from 8.5 to 10.5 (*lanes 5–7*, in supplemental Fig. S1*A*). A number of studies have shown that disaggregation of amyloid leads to the formation of monomers (21, 22). In our study we found that fibril disaggregation results in a mixture of monomers and oligomers. To investigate the proportion of the different structures released, we calculated the ratio of monomers/oligomers that were released upon disaggregation of fibrils at varying pH (6.5–10.5). For this purpose, soluble protein was fractionated by SEC, and the area of major peaks (peak 1, ~670 kDa (considered as oligomers), and peak 3, 15.7 kDa (considered as monomers despite that this peak may contain a mixture of monomers and dimers as shown by SDS-PAGE analysis)) was measured to calculate the ratio (supplemental Fig. S2A). As shown in supplemental Fig. S2*B*, the monomers/oligomers ratio appeared to increase as the pH approached basic (≥8.5), indicating that basic pH not only promotes release of soluble oligomers from fibrils but also to some extent destabilizes large oligomers into comparatively small oligomers (dimers through tetramers) and monomers.

Effects of NaCl Concentrations on Mcc Fibrils Disaggregation—Ionic strength is believed to play a key role in the assembly and stability of amyloid fibrils (17, 23). To investigate this, preformed Mcc fibrils were treated at various NaCl concentrations (0, 50, 150, 500, 750, and 1000 mM) in 50 mM PIPES, pH 6.5, for 2 h. Studies by sedimentation assay clearly revealed a significant increase in soluble Mcc at 0 and 50 mM NaCl (Fig. 3, *A* and *B*). Approximately 18% of the total fibrillar protein was released as soluble form at 0 mM NaCl. However, at higher concentrations of NaCl (150–1000 mM) no significant fibril dissolution was observed (Fig. 3*B*). Turbidity assay confirmed the sedimentation results, indicating that incubation in the absence of NaCl substantially decreases the relative quantity of large aggregates able to scatter light (Fig. 3*C*). Surprisingly, turbidity of fibrils incubated at 1000 mM NaCl showed a small but significant decreased signal compared with untreated control (*dashed line* in Fig. 3*C*) despite the sedimentation data, showing that soluble

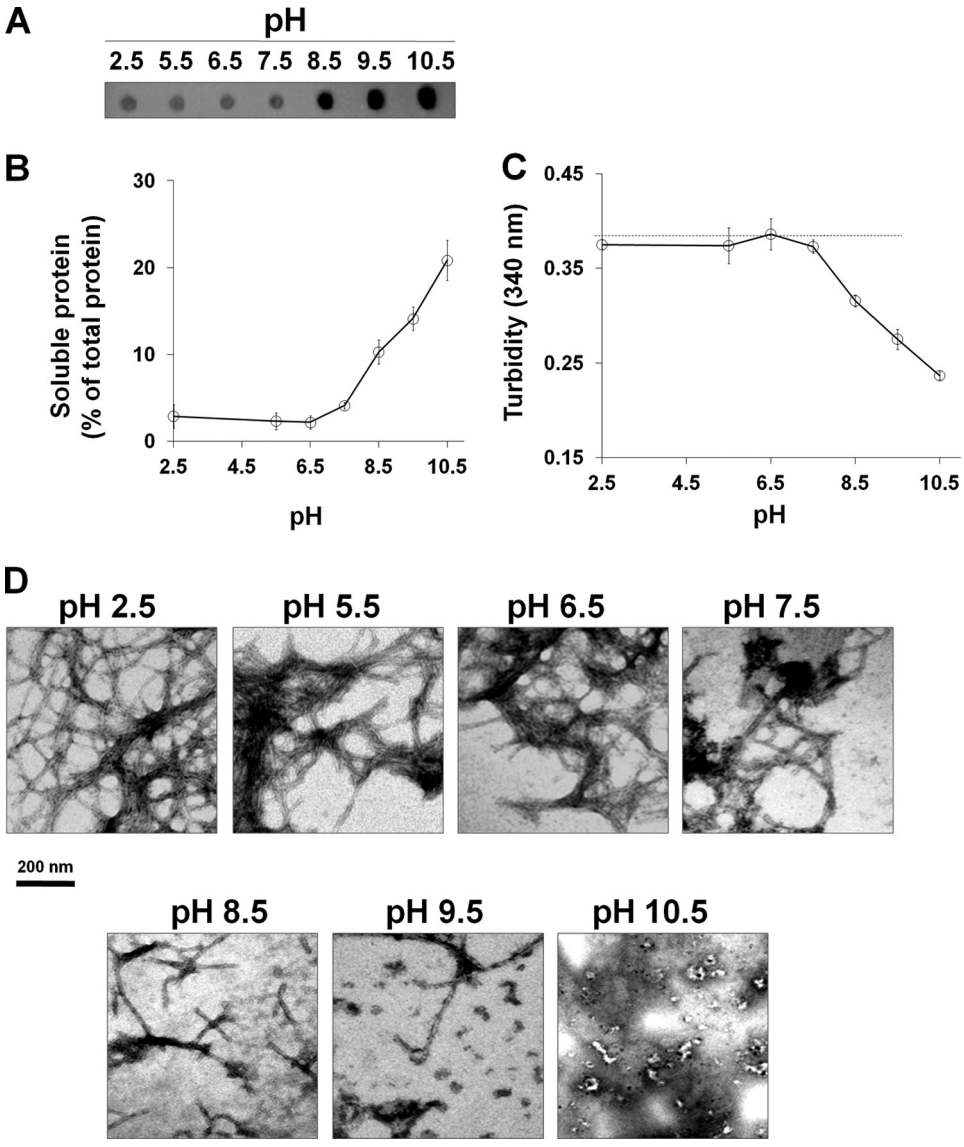

FIGURE 2. **Disaggregation of Mcc fibrils at varying pH values.** Mcc fibrils were prepared *in vitro* by incubating soluble Mcc at 400 μg/ml in 50 mM PIPES-NaOH, pH 6.5, 500 mM NaCl at 37 °C with agitation for 24 h and treated at different pH values as indicated for 2 h at 25 °C. Small aliquots were removed and centrifuged at 16,500 $\times$ *g* for 10 min, and supernatants were collected. *A*, shown is dot blot quantitation of soluble Mcc in supernatant. *B*, shown is a BCA analysis of soluble protein in supernatant after centrifugation. *C*, turbidity of samples of Mcc fibrils treated at different pH values for 2 h was checked by measuring absorbance at 340 nm. *D*, morphology of aggregates obtained after incubation at distinct pHs was examined by electron microscopy using a magnification of 150,000. The *dashed line* in *panel C* corresponds to turbidity of control, untreated Mcc fibrils. The *bar* in *panel D* represents 200 nm. *Error bars* represent $\pm$ S.D. of triplicate samples.

Mcc was not increased in the supernatant under these conditions (Fig. 3, *A* and *B*). This seemingly contradictory result could indicate that there was a partial disaggregation of large fibrils upon incubation with high salt concentration but that the released aggregates were large enough to remain in the pellet after centrifugation. To characterize the morphologies of species formed at lower NaCl concentrations, samples were examined by electron microscopy. Morphology of fibrils treated at NaCl concentrations (150–1000 mM) (data not shown) was indistinguishable from those of untreated fibrils (*top panel* in Fig. 3*D*). However, fibrils at low NaCl concentration (50 mM) appeared to disaggregate into more heterogeneous species predominately protofibrils and oligomers (*middle panel* in Fig. 3*D*). Such effect was more pronounced at 0 mM NaCl where oligomeric species were much more abundant (*bottom panel* in Fig. 3*D*). Consistently, SDS-PAGE analysis of soluble Mcc produced by incubation at 0 and 50 mM of NaCl showed an abundance of large oligomers (~100 to >260 kDa) and monomers through tetramers (*lanes 1* and *2* in supplemental Fig. S1*B*). However, higher NaCl concentrations (150–1000 mM) had no significant effect (*lanes 3–6* in supplemental Fig. S1*B*). These results clearly demonstrate that lower NaCl concentrations (≤50 mM) promote disassembly of fibril into smaller species.

Effects of Dilution on Mcc Fibrils Disaggregation—The concentration of the protein forming the fibrillar aggregates is another variable that may influence fibril stability by changing the equilibrium between fibrils and smaller aggregates. To study this possibility, we diluted preformed Mcc fibrils in 50 mM PIPES (pH 6.5), 500 mM NaCl. A progressive release of soluble Mcc from the fibrillar aggregates was observed upon

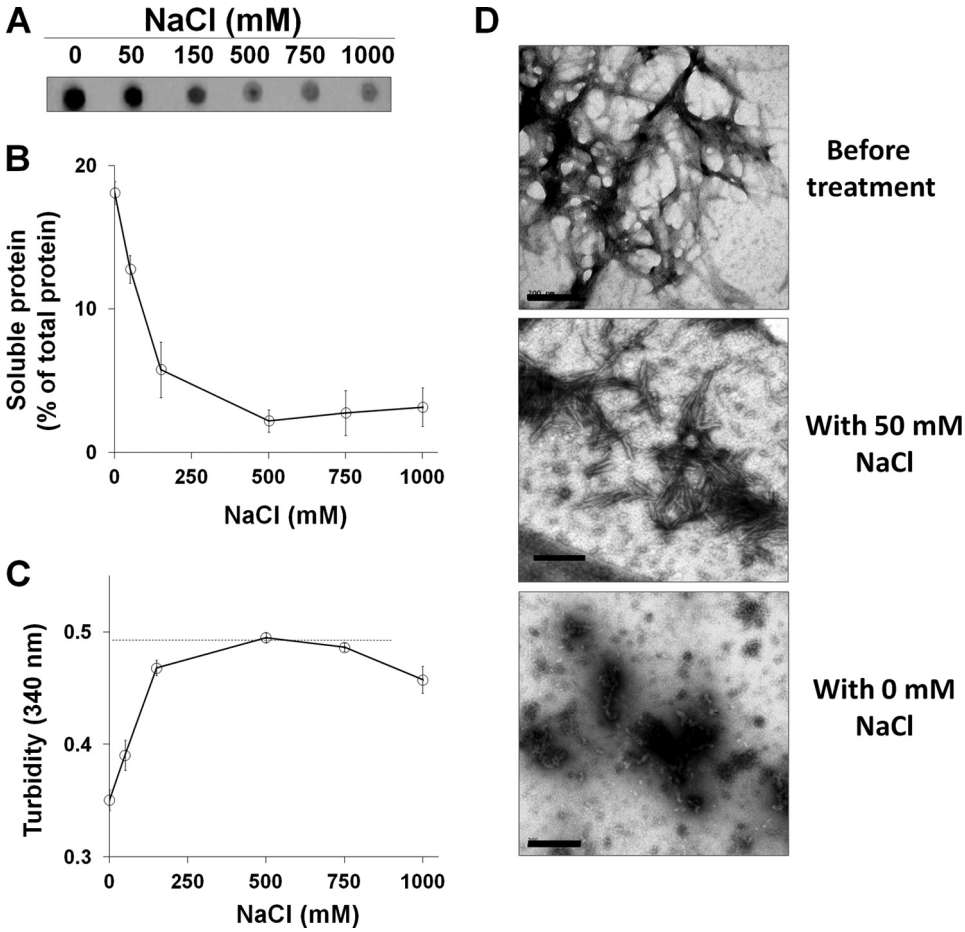

FIGURE 3. **Disaggregation of Mcc fibrils at varying NaCl concentrations.** Mcc fibrils were prepared *in vitro* by incubating soluble Mcc at 400 μg/ml in 50 mM PIPES-NaOH, pH 6.5, 500 mM NaCl at 37 °C with agitation for 24 h and treated at varying NaCl concentrations as indicated for 2 h at 25 °C. Small aliquots were removed and centrifuged at 16,500 × *g* for 10 min, and supernatants were collected. *A*, shown is a dot blot estimation of the quantity of soluble Mcc in supernatant. *B*, shown is BCA analysis of the percentage of soluble protein in supernatant after centrifugation. *C*, turbidity of samples of Mcc fibrils treated at varying NaCl concentrations for 2 h was checked by measuring absorbance at 340 nm. The *dashed line* in *panel C* corresponds to turbidity of untreated Mcc fibrils, as a control. *D*, morphologies of Mcc fibrils before (*top panel*) and after being treated at 50 (*middle panel*) and 0 mM NaCl (*bottom panel*) were examined by electron microscopy using a magnification of ×150,000. *Bars* in *panel D* represent 200 nm. *Error bars* represent ± S.D. of triplicate samples.

dilution (Fig. 4, *A* and *B*). We estimated that ~20% of the total fibrillar protein was recovered in the supernatant after incubation in buffer with the equivalent to a 10-fold dilution compared with the concentration in which the fibrils were produced. In this case the results of turbidity mirrored exactly those obtained by sedimentation (Fig. 4*C*). The morphologies of disaggregated species upon dilution (5–10-fold) were observed by electron microscopy. Consistent with our results with sedimentation and turbidity assays, electron microscopy clearly showed formation of smaller oligomeric species that co-existed with very thin fibers when aggregates were diluted 5-fold (*middle panel* in Fig. 4*D*) compared with untreated fibrils (*top panel* in Fig. 4*D*) The extent of disaggregation was much more pronounced at 10-fold dilution, where smaller oligomeric species could be clearly observed (*bottom panel* in Fig. 4*D*). SDS-PAGE analysis of soluble Mcc after dilution of fibrils 5- and 10-fold showed an increase of large oligomers (~100 to >260 kDa) and monomers through tetramers (supplemental Fig. S1*C*). Interestingly, the patterns of soluble Mcc species on SDS-PAGE upon 5- and 10-fold dilution of fibrils were similar to those obtained at basic pH (≥8.5) and at low NaCl concentrations (≤50 mM), which implies soluble proteins released under these conditions are of similar characteristics.

Size Distributions of Mcc Species Formed during Aggregation and upon Disaggregation of Mcc Fibrils—SEC has been widely used to characterize the distribution of amyloidogenic protein oligomers on the basis of their sizes. To gain insight into the sizes of Mcc species formed during Mcc aggregation and upon disaggregation of Mcc fibrils, we performed SEC studies. Aliquots (500 μl) from Mcc aggregation reaction before ($t = 0$ h, un-aggregated) and after incubation for different time points (6 and 12 h) were centrifuged at 16,500 × *g* for 10 min, and supernatants were subjected to SEC (Fig. 5*A*). Un-aggregated Mcc (0 h) revealed a single prominent peak (peak 3) by SEC (*top panel* in Fig. 5*A*) with estimated molecular masses of ~15.7 kDa. Considering the size, this peak corresponds to either a monomer with abnormally larger migration in SEC or a dimer. After 6 h of incubation a second heterogeneous peak (peak 2) was observed with estimated molecular masses of between 100 and 170 kDa (*middle panel* in Fig. 5*A*), which would correspond to Mcc oligomers containing between 12 and 20 monomers of the protein. Further incubation of the mixture led to the formation of larger

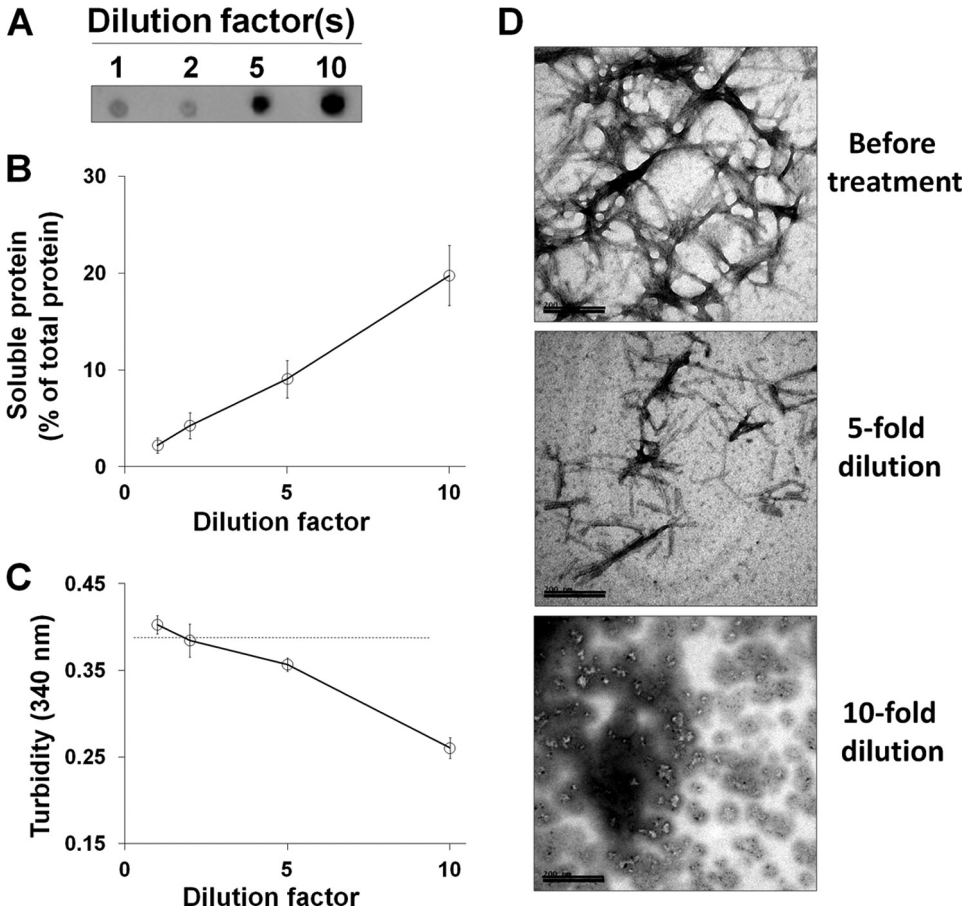

FIGURE 4. **Disaggregation of Mcc fibrils at varying dilutions.** Mcc fibrils were prepared *in vitro* by incubating soluble Mcc at 400 μg/ml in 50 mM PIPES-NaOH, pH 6.5, 500 mM NaCl at 37 °C with agitation for 24 h and incubated at different dilutions as indicated for 2 h at 25 °C. Small aliquots were removed and centrifuged at 16,500 × *g* for 10 min, and supernatants were collected. *A*, shown is an estimation by dot blot of soluble Mcc in the supernatant. *B*, shown is BCA analysis of soluble protein in supernatant after centrifugation. *C*, turbidity of samples of Mcc fibrils treated at different dilutions for 2 h was measured by registering the absorbance at 340 nm. The *dashed line* in *panel C* corresponds to turbidity of control, untreated Mcc fibrils. *D*, Morphologies of Mcc fibrils before (*top panel*) and after being treated at 5-fold (*middle panel*) and 10-fold dilution (*bottom panel*) were examined by electron microscopy using a magnification of ×150,000. *Bars* in *D* represent 200 nm. *Error bars* represent ± S.D. of triplicate samples.

assemblies as evident by the appearance of a new peak at the void volume (peak 1), corresponding to a molecular mass higher than 670 kDa. At this time we did not detect peak 2, suggesting the transient nature of these small oligomers. SEC analysis of Mcc aggregation was in accordance with morphologic characterization of Mcc aggregates by transmission electron microscopy (see Fig. 1*C*, for more details), where formation of oligomeric species (6 h) from un-aggregated Mcc (0 h) and then conversion into larger oligomeric/protofibrillar species could be observed in a time-dependent manner. SDS-PAGE of soluble Mcc after aggregation (up to 12 h) revealed formation of large oligomers, ~100 to >260 kDa and monomers through tetramers (<10 to ~30 kDa) (whole (*W*) in Fig. 5*D*). And SDS-PAGE analysis of peaks isolated by SEC after Mcc aggregation showed that peak 1 was enriched in SDS-resistant oligomers ~180 to >260 kDa, whereas peak 2 mainly contained species of ~100–160 kDa, and peak 3 was enriched in monomers as well as dimers (<10 to ~15 kDa) (Fig. 5*D*). Next, to study whether dissociation of Mcc fibrils under the conditions described before leads to the appearance of species with similar sizes, aliquots of Mcc fibrils were treated under our best dissolution condition (10-fold dilution in 0.1% NH_4OH, pH 10.5, 0 mM NaCl), where ~69% of total protein was found to be in soluble form as confirmed by BCA assay (data not shown), and soluble protein was characterized by SEC. The starting point of this experiment was a solution containing Mcc fibrils formed by incubation at 37 °C in aggregation buffer (in 50 mM PIPES-NaOH, pH 6.5, 500 mM NaCl) for 24 h. Chromatographic separation of this material after centrifugation to remove large aggregates showed no detectable peaks (*top panel* in Fig. 5*B*). Interestingly, supernatant obtained after disaggregation of Mcc fibrils during 2 h gave three peaks (peak 3, ~15.7 kDa; peak 2, ~100–170 kDa; peak 1, ~ 670kDa) by SEC (*bottom panel* in Fig. 5*B*). The remarkable size equivalency of these peaks with those observed during Mcc aggregation led us to suggest that the species formed during aggregation and upon disaggregation are likely very similar. Next we sought to characterize by transmission electron microscopy the morphologies of the Mcc species released upon fibril disaggregation and isolated by SEC (Fig. 5*C*). Peak 3 fraction showed no distinguishable structures (*right panel* in Fig. 5*C*). The peak 2 fraction contained mainly oligomers in abundance with varying diameters (~3–60 nm) (*center panel* in Fig. 5*C*). Morphologies of Mcc species in peak 1 fraction showed the abundance of proto-

fibrillar structures with lengths of ~100–300 nm (*left panel* in Fig. 5*C*). Interestingly, size distribution by SEC and morphologic analysis by transmission electron microscopy of Mcc species released after disaggregation of Mcc fibrils revealed a clear resemblance to the species formed during Mcc aggregation (Fig. 5*A* and Fig. 1*C*), which highlights the notion that both pathways share the formation of common species. This was further confirmed by SDS-PAGE analysis. Indeed, SDS-PAGE

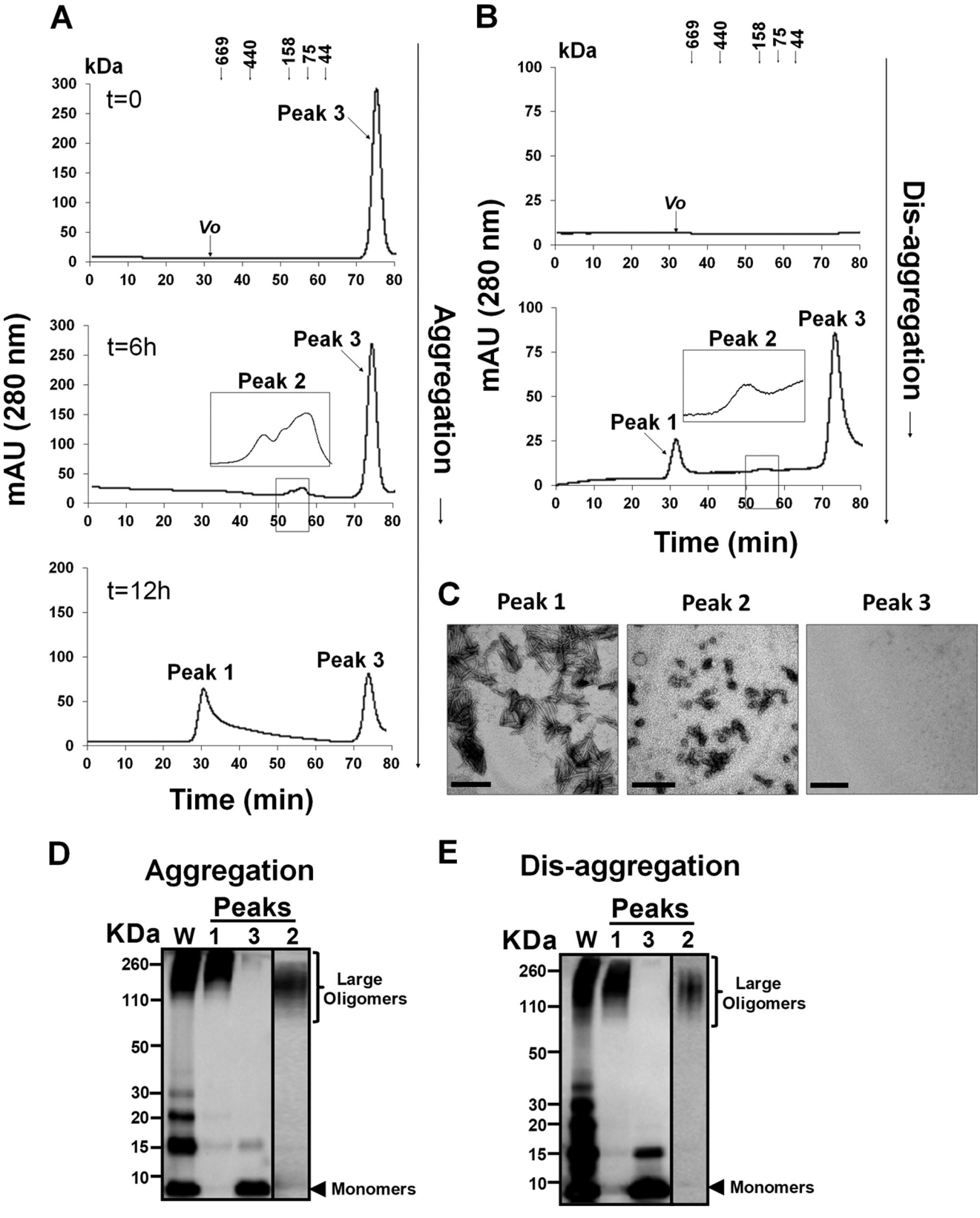

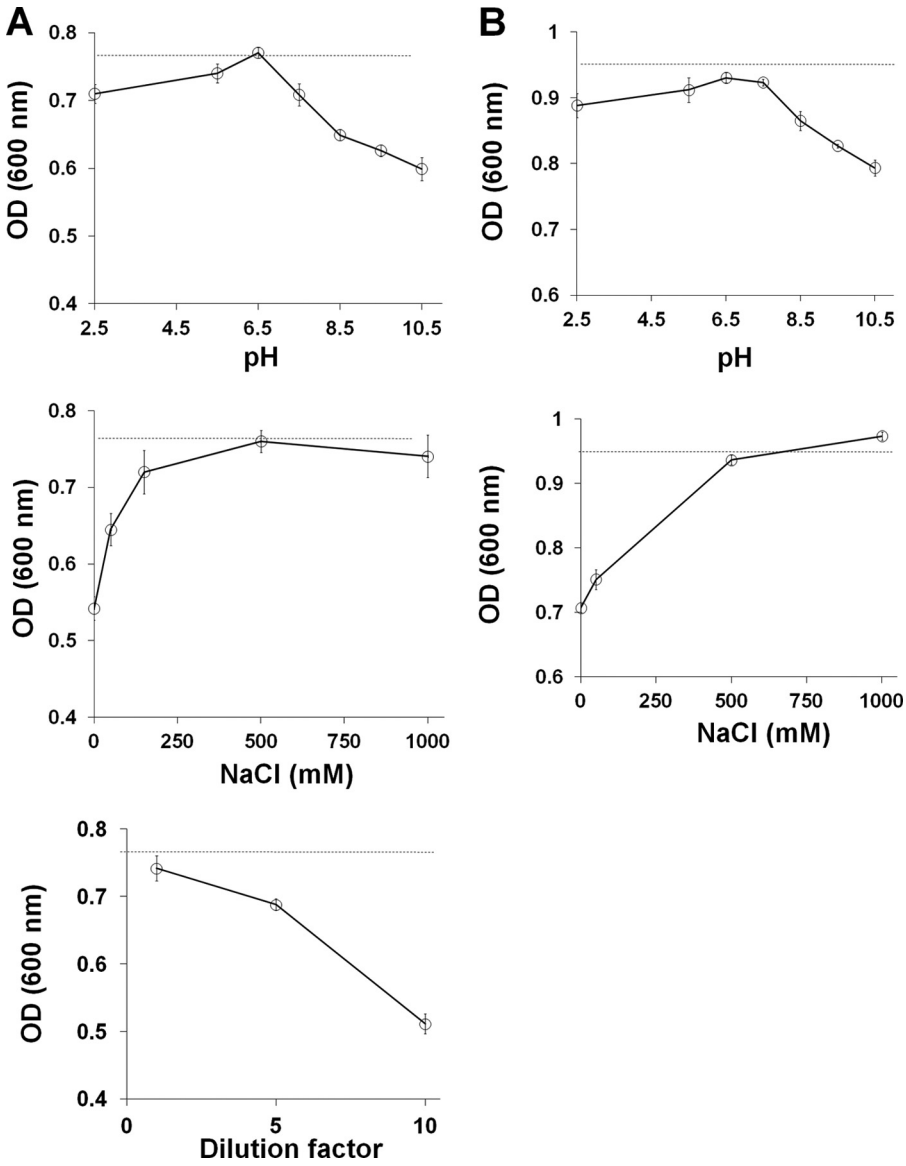

FIGURE 6. **Cytotoxicity of disaggregated Mcc fibrils at various conditions.** *A*, Mcc fibrils were prepared *in vitro* by incubating soluble Mcc at 400 μg/ml in 50 mM PIPES-NaOH, pH 6.5, 500 mM NaCl at 37 °C with agitation for 24 h. For disaggregation, samples of Mcc fibrils were incubated for 2 h at 25 °C under different conditions, including various pH (*top panel*), NaCl concentrations (*center panel*), and dilutions (*bottom panel*). *B*, Mcc fibrils were collected from the culture medium of bacteria producing Mcc, cultivated up to the stationary phase. *In vivo* produced Mcc fibrils were then treated by incubation for 2 h at 25 °C with different pH (*top panel*) and NaCl concentrations (*bottom panel*). In both *A* and *B*, after treatment, samples were incubated with sensitive bacteria for 16 h at 37 °C, and cytotoxicity was evaluated by measuring the absorbance of the culture at 600 nm (*OD (600 nm)*). For each condition, control samples included the addition to the bacteria culture of buffers at the same pH and NaCl concentrations as in the experimental groups. *Dashed lines* correspond to untreated Mcc fibrils, used as controls. *Error bars* represent ± S.D. of triplicate samples.

of isolated SEC peak fractions of soluble Mcc upon fibrils disaggregation showed species of similar molecular weights to those observed for Mcc aggregation: peak 1, ~180 to >260 kDa; peak 2, 100–160 kDa; peak 1, <10 to ~15 kDa (Fig. 5*E*). Again these results confirmed that species formed during aggregation and disaggregation are of similar molecular weights.

Disaggregation of Mcc Fibrils Releases Toxic Species—Soluble oligomers of Mcc have been reported to be highly toxic to bac-

FIGURE 5. **Characterization of Mcc aggregation and disaggregation by size exclusion chromatography and electron microscopy.** *A*, for Mcc aggregation, soluble protein at 400 μg/ml in 50 mM PIPES-NaOH, pH 6.5, 500 mM NaCl was incubated at 37 °C with agitation for 0 (*top panel*), 6 (*middle panel*), and 12 h (*bottom panel*). After incubation, an aliquot of 500 μl was removed at each time point and centrifuged at 16,500 × *g* for10 min, and supernatants were fractionated by SEC. *mAU*, milliabsorbance units. *B*, Mcc fibrils disaggregation was carried out by diluting preformed fibrils 10-fold in 0.1% NH_4OH, pH 10.5, 0 mM NaCl for 2 h at 25 °C. After incubation, the sample was centrifuged at 16,500 × *g* for 10 min, and the resultant supernatant before (*top panel*) and after disaggregation (*bottom panel*) was subjected to SEC. The elution profiles were detected by the absorbance at 280 nm. The *insets* in *panels A* and *B* show zoomed views for the part of chromatograms corresponding to peak 2. The elution profiles of calibration standards are indicated by *arrows* (in kDa) (*panel A* and *B*). *C*, morphologies of Mcc species fractionated in panel *B* were examined by electron microscopy; peak 1 (*left*), peak 2 (*center*), and peak 3 (*right*). *D* and *E*, shown are immunoblots of samples used in *panel A* (aggregation) and *panel B* (disaggregation) before and after SEC separation. Soluble Mcc species formed at 12 h of aggregation at 37 °C (whole (*W*)) and peak fractions (*1–3*) (*panel D*) and soluble species formed after disaggregation of Mcc fibrils (whole) and peaks fractions (*1–3*) obtained after SEC fractionation (*panel E*) were resolved by SDS-PAGE and immunoblotted with Mcc specific antibody. *Scale bars* represent 200 nm.

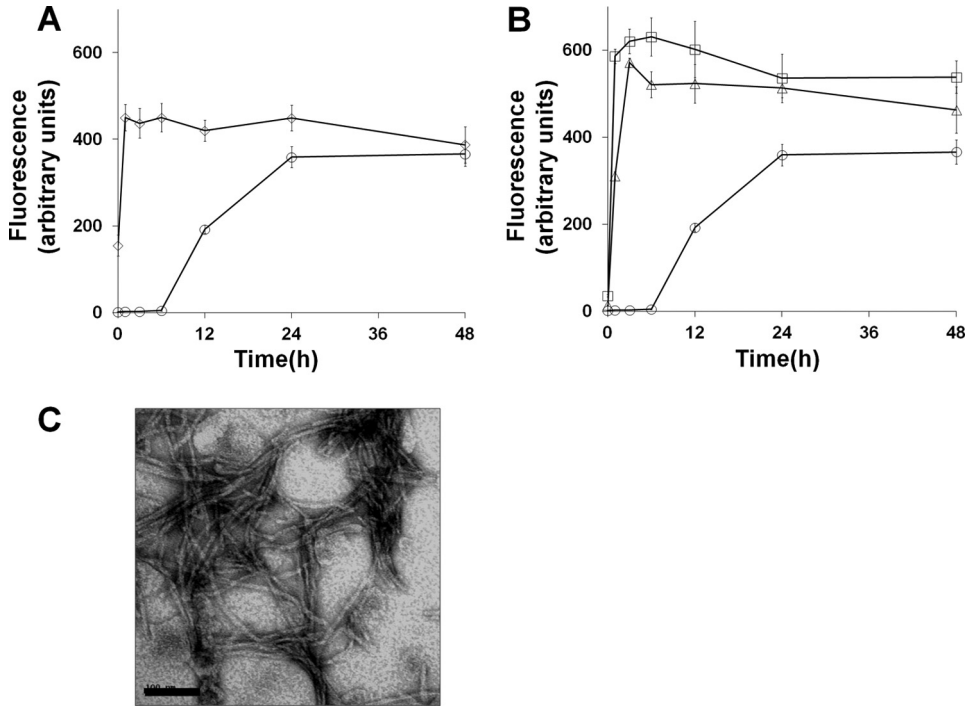

FIGURE 7. **Released soluble Mcc oligomers aggregate faster and seed aggregation of fresh soluble Mcc.** Preformed Mcc fibrils (400 μg/ml) produced as indicated in Figs. 2–5 were disaggregated by diluting 10-fold in 50 mM sodium borate buffer, pH 10.5, 0 mM NaCl, and incubating the samples under these conditions for 2 h at 25 °C. After incubation, the sample was centrifuged at 16,500 × *g* for 10 min, and the resultant supernatant was concentrated and resuspended for reassembly in 50 mM PIPES, pH 6.5, 500 mM NaCl. *A*, aliquots of disaggregated samples were incubated at 37 °C for different times (◇), and amyloid formation was measured by ThT binding assay along with a control consisting of fresh soluble Mcc (○) incubated under the same conditions. *B*, to study the ability of disaggregated Mcc fibrils to seed Mcc aggregation, fresh soluble Mcc (400 μg/ml) was allowed to aggregate in 50 mM PIPES, pH 6.5, 500 mM NaCl at 37 °C for 48 h either alone (○) or with 20 (△) or 40 μg/ml (□) of Mcc oligomers released from treated fibrils. Aliquots were removed at the indicated time points, and ThT assay was carried out. *C*, morphology of Mcc fibrils formed after reassembly of disaggregated species was examined by electron microscopy using a magnification of ×150,000. *Bars* in *C* represent 200 nm. *Error bars* represent ± S.D. of triplicate samples.

terial cells, whereas amyloid fibrils are little or non-toxic (13). Having established the conditions to produce a partial disaggregation of Mcc fibrils, we sought to examine the toxicity of Mcc oligomers released from disaggregated fibrils. We determined the toxicity of aliquots withdrawn from untreated Mcc fibrils (Fig. 6*A*, *dashed lines*) and fibrils treated at different conditions: pH 2.5–10.5 (Fig. 6*A*, *top panel*); NaCl (0–1000 mM) (Fig. 6*A*, *center panel*); dilutions (up to 10-fold) (Fig. 6*A*, *bottom panel*). Toxicity was measured by incubating the solution containing Mcc with sensitive bacteria and assessing the bacterial growth after 16 h of incubation at 37 °C. Bacterial growth was estimated by measuring the absorbance of the culture at 600 nm (A_{600}). Fibrils treated with basic pH (≥8.5) showed significant toxicity (Fig. 6*A*, *top panel*). The increase in Mcc toxicity was directly proportional to the amount of soluble Mcc released from the fibrils under these conditions (see Fig. 2, *A* and *B*). Similar results were observed in the experiments in which fibrils were disaggregated by treatment with buffer containing low salt concentrations (0 and 50 mM NaCl) and upon high dilution (5- and 10-fold) (Fig. 6*A*, *center* and *bottom panels*, respectively). Again, the extent of increase in toxicity was directly proportional to the magnitude to which soluble oligomers were released from the fibrils under these conditions. The results clearly suggest that soluble Mcc released from the fibrils was toxic, indicating that non-toxic fibrillar aggregates might be considered as a reservoir of toxic oligomers.

In Vivo Produced Mcc Fibrils Can Be Disaggregated to Release Toxic Species—Up to now all studies have been done with Mcc fibrils polymerized *in vitro* using purified protein. As we have reported before, Mcc also forms amyloid fibrils under *in vivo* conditions during the bacterial life cycle (13). Because fibrils formed *in vivo* may be more stable and exhibit distinct properties than those produced *in vitro*, we carried out a similar study with Mcc fibrils polymerized *in vivo*. For this purpose, Mcc fibrils were taken from bacterial culture producing Mcc at the stationary phase by centrifugation of the medium. Toxicity was measured for aliquots of untreated fibrils (Fig. 6*B*, *dashed lines*) or fibrils treated at different pH values (2.5–10.5) (Fig. 6*B*, *top panel*) and at different NaCl concentrations (0–1000 mM) (Fig. 6*B*, *bottom panel*). As was observed with Mcc fibrils polymerized *in vitro* (Fig. 6*A*), *in vivo* produced material was also able to release toxic Mcc oligomeric species upon conditions that promote fibril disaggregation.

Released Soluble Mcc Aggregates Faster and Seeds Aggregation of Fresh Soluble Mcc—Next we investigated whether soluble protein released from fibrils upon treatment at high pH, low salinity, or after dilution can re-assemble into mature fibrils. For this experiment, fibrils were disaggregated by diluting 10-fold in 50 mM sodium borate, pH 10.5, 0 mM NaCl. Released soluble Mcc protein was concentrated and allowed to aggregate by changing pH and ionic strength (pH 6.5 and 500 mM NaCl). As clearly shown in Fig. 7*A*, released soluble Mcc protein (400

μg/ml) quickly assembled into amyloid fibrils as measured by ThT assay, which was confirmed by electron microscopy (Fig. 7*C*). Interestingly, the kinetic of aggregation of disaggregated fibrils was substantially faster than fresh soluble Mcc incubated under the same condition (Fig. 7*A*), clearly suggesting that the product of Mcc fibril disaggregation was an oligomeric structure that was an on-pathway intermediate in amyloid formation. This conclusion was further supported by an experiment in which we assessed the seeding activity of disaggregated Mcc fibrils. The addition of released Mcc oligomers (20 or 40 μg/ml) shortened dramatically the lag phase of fresh soluble Mcc aggregation in a dose-dependent manner (Fig. 7*B*).

DISCUSSION

The misfolding and aggregation of proteins into fibrillar amyloid deposits is a hallmark process in various diseases, collectively called protein misfolding disorders, which include some highly prevalent illnesses such as Alzheimer disease, type 2 diabetes, Parkinson disease, and also more than 20 other rarer disorders (24–27). Interestingly, the notion that misfolded amyloid aggregates are exclusively associated to diseases has changed dramatically over the past 10 years by the discovery that many proteins can naturally form amyloid structures, which in some cases are associated to changes in the biological function of the proteins (22, 28–31). Moreover, the elegant studies from Dobson and co-workers (32–34) have demonstrated that virtually any protein can be made to misfold and aggregate forming amyloid fibrils under appropriate conditions, leading to the concept that amyloid may be the primordial folding of proteins.

In a previous study we demonstrated that the biological activity of the bacterial toxin microcin E492 is modulated *in vivo* by the formation of amyloid fibrils in the bacterial culture (13). Interestingly, the mechanism of Mcc amyloid formation and the structure and biochemical properties of the end product and intermediates in the process of misfolding and aggregation are indistinguishable from the disease-associated amyloids. In this study we show that Mcc fibrils polymerized *in vitro* and *in vivo* harbor biologically active oligomeric species that can be released from the fibrils upon changing the environmental conditions. Indeed relatively small changes in pH, NaCl concentrations, and dilution resulted in the release of soluble Mcc, which retains its cytotoxic activity intact. This data suggest that the process of amyloid formation is highly dynamic and that biologically inert Mcc fibrils can be a reservoir of toxic soluble oligomeric structures. Although the specific Mcc conformation that is responsible for cytotoxicity is still unclear, several lines of evidence indicate that Mcc exert its toxicity by forming pores on the bacterial cell membrane (6, 8), which requires the oligomerization of Mcc monomers. Strikingly, the current view in protein misfolding diseases is that the toxic species might be oligomeric pore-like structures that may cause cell damage by permeabilizing membranes and altering cellular homeostasis (15, 35, 36). Indeed, amyloid-β and α-synuclein annular oligomers associated to the pathogenesis of Alzheimer and Parkinson disease, respectively, were shown to resemble the cytolytic β-barrel pore-forming bacteriotoxins (19, 37), suggesting that a common structure could be responsible for toxicity in both natural and pathological misfolded oligomers. Moreover, compelling evidence accumulated in the past several years strongly suggests that mature amyloid fibrils may not be the toxic structures responsible for cellular degeneration in protein misfolding diseases but rather may be considered as inert end products or even as a protective mechanism to sequester the toxic oligomeric intermediates (15). The extrapolation of our results to disease-associated misfolded aggregates suggests that large amyloid fibrils accumulated in the tissue of patients affected by misfolding diseases may act as a depot of toxic soluble oligomers.

Microcins have been proposed to play a key role in the maintenance of homeostasis in the intestinal microbial ecosystem (5, 38). It appears that Mcc-producing bacteria secrete soluble Mcc, which upon oligomerization form toxic pores to kill competing bacteria. Once Mcc-producing bacteria have prevailed over competitors, soluble Mcc gets assembled into amyloid fibrils resulting in the sequestration of toxic species into inert structures. These aggregates accumulate over time and may constitute a depot of toxic oligomers that can be released when environmental conditions change and competition arises. In conclusion, our results suggest that a dynamic and reversible process of Mcc aggregation and disaggregation may regulate the production or release of active bacteriocin and contribute to maintain homeostasis in the microbial ecosystem.

Acknowledgment—We thank Dr. Rosalba Lagos (University of Chile) for providing bacteria producing microcin.

REFERENCES

1. Riley, M. A. (1998) Molecular mechanisms of bacteriocin evolution. *Annu. Rev. Genet.* **32,** 255–278
2. Riley, M. A., Goldstone, C. M., Wertz, J. E., and Gordon, D. (2003) A phylogenetic approach to assessing the targets of microbial warfare. *J. Evol. Biol.* **16,** 690–697
3. Riley, M. A., and Wertz, J. E. (2002) Bacteriocin diversity. Ecological and evolutionary perspectives. *Biochimie* **84,** 357–364
4. de Lorenzo, V. (1984) Isolation and characterization of microcin E492 from *Klebsiella pneumoniae*. *Arch. Microbiol.* **139,** 72–75
5. de Lorenzo, V., Martínez, J. L., and Asensio, C. (1984) Microcin-mediated interactions between *Klebsiella pneumoniae* and *Escherichia coli* strains. *J. Gen. Microbiol.* **130,** 391–400
6. Destoumieux-Garzón, D., Thomas, X., Santamaria, M., Goulard, C., Barthélémy, M., Boscher, B., Bessin, Y., Molle, G., Pons, A. M., Letellier, L., Peduzzi, J., and Rebuffat, S. (2003) Microcin E492 antibacterial activity. Evidence for a TonB-dependent inner membrane permeabilization on *Escherichia coli*. *Mol. Microbiol.* **49,** 1031–1041
7. Baquero, F., and Moreno, F. (1984) *FEMS Microbiol. Lett.* **23,** 117–124
8. de Lorenzo, V., and Pugsley, A. P. (1985) Microcin E492, a low molecular weight peptide antibiotic that causes depolarization of the *Escherichia coli* cytoplasmic membrane. *Antimicrob. Agents Chemother.* **27,** 666–669
9. Lagos, R., Wilkens, M., Vergara, C., Cecchi, X., and Monasterio, O. (1993) Microcin E492 forms ion channels in phospholipid bilayer membrane. *FEBS Lett.* **321,** 145–148
10. de Lorenzo, V. (1985) Factors affecting microcin E492 production. *J. Antibiot.* **38,** 340–345
11. Corsini, G., Baeza, M., Monasterio, O., and Lagos, R. (2002) The expression of genes involved in microcin maturation regulates the production of active microcin E492. *Biochimie* **84,** 539–544
12. Orellana, C., and Lagos, R. (1996) The activity of microcin E492 from *Klebsiella pneumoniae* is regulated by a microcin antagonist. *FEMS Microbiol. Lett.* **136,** 297–303

13. Bieler, S., Estrada, L., Lagos, R., Baeza, M., Castilla, J., and Soto, C. (2005) Amyloid formation modulates the biological activity of a bacterial protein. *J. Biol. Chem.* **280,** 26880–26885
14. Hetz, C., Bono, M. R., Barros, L. F., and Lagos, R. (2002) Microcin E492, a channel-forming bacteriocin from *Klebsiella pneumoniae*, induces apoptosis in some human cell lines. *Proc. Natl. Acad. Sci. U.S.A.* **99,** 2696–2701
15. Caughey, B., and Lansbury, P. T. (2003) Protofibrils, pores, fibrils, and neurodegeneration. Separating the responsible protein aggregates from the innocent bystanders. *Annu. Rev. Neurosci.* **26,** 267–298
16. Wray, W., Boulikas, T., Wray, V. P., and Hancock, R. (1981) Silver staining of proteins in polyacrylamide gels. *Anal. Biochem.* **118,** 197–203
17. Raman, B., Chatani, E., Kihara, M., Ban, T., Sakai, M., Hasegawa, K., Naiki, H., Rao ChM., and Goto, Y. (2005) Critical balance of electrostatic and hydrophobic interactions is required for β2-microglobulin amyloid fibril growth and stability. *Biochemistry* **44,** 1288–1299
18. Shammas, S. L., Knowles, T. P., Baldwin, A. J., Macphee, C. E., Welland, M. E., Dobson, C. M., and Devlin, G. L. (2011) Perturbation of the stability of amyloid fibrils through alteration of electrostatic interactions. *Biophys. J.* **100,** 2783–2791
19. Lashuel, H. A., Hartley, D., Petre, B. M., Walz, T., and Lansbury, P. T., Jr. (2002) *Nature* **418,** 291
20. Lashuel, H. A., Petre, B. M., Wall, J., Simon, M., Nowak, R. J., Walz, T., and Lansbury, P. T., Jr. (2002) α-Synuclein, especially the Parkinson disease-associated mutants, forms pore-like annular and tubular protofibrils. *J. Mol. Biol.* **322,** 1089–1102
21. Nichols, M. R., Moss, M. A., Reed, D. K., Cratic-McDaniel, S., Hoh, J. H., and Rosenberry, T. L. (2005) Amyloid-β protofibrils differ from amyloid-β aggregates induced in dilute hexafluoroisopropanol in stability and morphology. *J. Biol. Chem.* **280,** 2471–2480
22. Maji, S. K., Perrin, M. H., Sawaya, M. R., Jessberger, S., Vadodaria, K., Rissman, R. A., Singru, P. S., Nilsson, K. P., Simon, R., Schubert, D., Eisenberg, D., Rivier, J., Sawchenko, P., Vale, W., and Riek, R. (2009) Functional amyloids as natural storage of peptide hormones in pituitary secretory granules. *Science* **325,** 328–332
23. Sikkink, L. A., and Ramirez-Alvarado, M. (2008) Salts enhance both protein stability and amyloid formation of an immunoglobulin light chain. *Biophys. Chem.* **135,** 25–31
24. Soto, C. (2001) Protein misfolding and disease. Protein refolding and therapy. *FEBS Lett.* **498,** 204–207
25. Soto, C. (2003) Unfolding the role of protein misfolding in neurodegenerative diseases. *Nat. Rev. Neurosci.* **4,** 49–60
26. Dobson, C. M. (1999) Protein misfolding, evolution, and disease. *Trends Biochem. Sci.* **24,** 329–332
27. Carrell, R. W., and Lomas, D. A. (1997) Conformational disease. *Lancet* **350,** 134–138
28. Chiti, F., and Dobson, C. M. (2006) Protein misfolding, functional amyloid, and human disease. *Annu. Rev. Biochem.* **75,** 333–366
29. Fowler, D. M., Koulov, A. V., Balch, W. E., and Kelly, J. W. (2007) Functional amyloid. From bacteria to humans. *Trends Biochem. Sci.* **32,** 217–224
30. Badtke, M. P., Hammer, N. D., and Chapman, M. R. (2009) Functional amyloids signal their arrival. *Sci. Signal.* **2,** pe43
31. Fowler, D. M., Koulov, A. V., Alory-Jost, C., Marks, M. S., Balch, W. E., and Kelly, J. W. (2006) Functional amyloid formation within mammalian tissue. *PLoS. Biol.* **4,** e6
32. Chiti, F., Webster, P., Taddei, N., Clark, A., Stefani, M., Ramponi, G., and Dobson, C. M. (1999) Designing conditions for in vitro formation of amyloid protofilaments and fibrils. *Proc. Natl. Acad. Sci. U.S.A.* **96,** 3590–3594
33. Chiti, F., Bucciantini, M., Capanni, C., Taddei, N., Dobson, C. M., and Stefani, M. (2001) Solution conditions can promote formation of either amyloid protofilaments or mature fibrils from the HypF N-terminal domain. *Protein Sci.* **10,** 2541–2547
34. Zurdo, J., Guijarro, J. I., Jiménez, J. L., Saibil, H. R., and Dobson, C. M. (2001) Dependence on solution conditions of aggregation and amyloid formation by an SH3 domain. *J. Mol. Biol.* **311,** 325–340
35. Lashuel, H. A., and Lansbury, P. T., Jr. (2006) Are amyloid diseases caused by protein aggregates that mimic bacterial pore-forming toxins? *Q. Rev. Biophys.* **39,** 167–201
36. Lashuel, H. A. (2005) Membrane permeabilization: a common mechanism in protein misfolding diseases. *Sci. Aging Knowledge Environ.* **2005,** e28
37. Hotze, E. M., Heuck, A. P., Czajkowsky, D. M., Shao, Z., Johnson, A. E., and Tweten, R. K. (2002) Monomer-monomer interactions drive the prepore to pore conversion of a β-barrel-forming cholesterol-dependent cytolysin. *J. Biol. Chem.* **277,** 11597–11605
38. Savage, D. C. (1977) Microbial ecology of the gastrointestinal tract. *Annu. Rev. Microbiol.* **31,** 107–133